Received: 29 May 2023 | Revised: 8 December 2023 | Accepted: 28 December 2023

DOI: 10.1002/qua.27358

RESEARCH ARTICLE

International Journal of Quantum Chemistry WILEY

The confined helium atom: An information–theoretic approach

C. R. Estañón[1] | H. E. Montgomery Jr.[2] | J. C. Angulo[3,4] | N. Aquino[1]

[1]Departamento de Física, Universidad Autónoma Metropolitana-Iztapalapa, Ciudad de Mexico, Mexico

[2]Chemistry Program, Centre College, Danville, Kentucky, USA

[3]Departamento de Física Atómica, Molecular y Nuclear, Universidad de Granada, Granada, Spain

[4]Instituto Carlos I de Física Teórica y Computacional, Universidad de Granada, Granada, Spain

Correspondence
N. Aquino, Departamento de Física, Universidad Autónoma Metropolitana-Iztapalapa, Av. San Rafael Atlixco 186, Col. Vicentina, CP 09340 CDMX, Mexico.
Email: naa@xanum.uam.mx

Funding information
Universidad de Granada; Junta de Andalucía

Abstract

In this article, we study the helium atom confined in a spherical impenetrable cavity by using informational measures. We use the Ritz variational method to obtain the energies and wave functions of the confined helium atom as a function of the cavity radius r_0. As trial wave functions we use one uncorrelated function and five explicitly correlated basis sets in Hylleraas coordinates with different degrees of electronic correlation. We computed the Shannon entropy, Fisher information, Kullback–Leibler entropy, Tsallis entropy, disequilibrium and Fisher–Shannon complexity, as a function of r_0. We found that these entropic measures are sensitive to electronic correlation and can be used to measure it. As expected these entropic measures are less sensitive to electron correlation in the strong confinement regime ($r_0 < 1$ a.u.).

KEYWORDS
confined helium atom, disequilibrium, Fisher information, Fisher–Shannon complexity, Kullback–Leibler entropy, Shannon entropy, Tsallis entropy

1 | INTRODUCTION

Spatially confined quantum systems have become the subject of increasing attention because when a very high pressure is exerted on a physical system, its energy levels increase rapidly. However, not all of them grow with the same rate, and this results in the filling of the energy levels that may differ significantly from those of the compression-free system. As a consequence its physical properties can change drastically with high pressure. Notable changes are found in electronic structure, emission and absorption frequencies, half-lives of excited states, selection rules, polarizability, electronic affinity, chemical and ionization potential and so forth. Confined quantum systems can be used to model a wide variety of problems in physics and chemistry such as: atoms trapped in cavities, in zeolite channels, in fullerenes, the electronic structure of atoms and molecules subjected to high external pressures, the behavior of the specific heat of a monocrystal solid under high pressure, in the study of the proton–deuteron transformation as a source of energy in dense stars, in the theory of white dwarf stars, phase transitions caused by compression as in the collapse of the chemical bonding of H_2 [1–9] and so forth. This growing interest is also due to the fabrication of quantum systems of nanometric sizes with potential technological applications such as in quantum wires, dots and wells [10, 11].

In 1937 Michels et al. [12] studied the variation of the polarizability of the hydrogen atom subjected to high external pressures. They proposed a model in which a hydrogen atom is confined inside an impenetrable spherical cavity with the nucleus clamped in the center of a sphere of radius r_0. This model is known as the confined hydrogen atom (CHA) [7, 13–16], and has been used to study how some physical properties behave in terms of pressure, such as: the hyperfine separation, given by the Fermi contact term, and the nuclear magnetic screening of the ground state. Emission frequencies, as well as the half-lives of some excited states [17, 18], and electronic properties of multi-electron atoms have been studied with it. The model has been extended to cavities of shapes other than spherical to study atoms and molecules trapped inside cavities.

After the confined hydrogen atom, the next most studied confined atom is the helium atom. Confined helium–like atoms are the simplest confined many-electron atoms, consisting of a nucleus with nuclear charge Z and two electrons. It is now when the electron–electron repulsion appears, which

is responsible for the fact that the time-independent Schrödinger equation does not have an exact solution. The first to study the ground state of confined helium system were Ten Seldam and De Groot in 1952 [19]. They used the nonlinear variational method and a trial wave function that explicitly contained the electronic correlation. Gimarc [20] used the same method but employing 5 different trial wave functions, one of which produced results similar to the HF calculations, and two of them explicitly included electronic correlation. Subsequent to Gimarc, different methods have been developed, for example, Hartree–Fock [21], Roothaan–Hartree–Fock [22], Configuration Interaction [23], time independent perturbation theory [24], linear and non-linear variational method [24–35], Lagrange mesh method [36], B–splines [37], variational quantum Monte Carlo [38, 39] and density functional theory [40–42]. Most of these studies have been devoted to the total energy calculations, correlation energy due to the radial and angular contribution of trial wave functions [31, 32], polarizability, critical cage radius and so forth, as a function of the confining radius. Subsequent work has been devoted to the study of low energy excited states $1sns^{1,3}S$, $1s2p^{1,3}P$, $1s3d^{1,3}D$, and other excited states [22, 37, 39, 43–47].

In information theory, entropy is a measure of the uncertainty associated with a random variable. In 1948 Claude E. Shannon introduced an information–theoretic measure, now known as the Shannon entropy [48], to quantify the expected value of the information contained in a message. Another important measure of information is Fisher information. In 1920 Fisher information [49] of a probability distribution was introduced. These two measures of information are classical, both quantities having their quantum counterparts. In addition, Quantum Information Theory (QIT) has gained interest due to its applications in quantum computation [50], chemical reactivity [51], atoms [52–54] and molecules [55], in the derivation of equations governing physics, [56–58], [59], image retrieval and indexing [60], machine learning [61], seismology [62], biological imaging [63] and so forth.

Information theory has been used in the study of one-, two-, and three-dimensional (1D, 2D and 3D) systems [64–70], in free systems and in systems subject to spatial confinement. As examples, we mention the study of free and spatially confined hydrogen and helium atoms [35, 41, 71–76].

As discussed in [77], in recent years a variety of complexity measures have been defined and applied to the study of systems in physical, biological, mathematical, computer science and so forth. These quantities are obtained from density functionals and expectation values of probability densities [73, 78–82].

Each complexity measure is directly related to information entropies and this allows us to determine global or local features of the probability density. For example: a global-local measure is described by the Fisher–Shannon complexity which relates the Shannon entropic power to the Fisher entropy, with the Fisher entropy providing a local measure of the probability density and the Shannon entropic power providing a global measure [53, 83–85].

The objective of this work is to obtain information about the level of correlation, beyond simply considering the correlation energy, by using various information theoretic measures and to find out which of them are more or less 'sensitive', as indicators of the level of correlation incorporated into the wave function. We use the Ritz variational method to obtain the energies and wave functions. Five functions with different degree of correlation were chosen as trial wave functions, the largest being an expansion in Hylleraas coordinates with 70 terms.

The work is organized as follows: In Section 2, we briefly describe the confined helium system, its solutions by the variational method and the informational measures used in this work: manely the Shannon entropy, Fisher information, Tsallis, disequilibrium, Kullback–Leibler entropies, and the Fisher–Shannon complexity. In Section 3 the respective numerical results are provided and discussed. Section 4 is devoted to the analysis the information-theoretic mesaures. the appendix shows the relationship of correlation energy and information–theoretic measures. Finally, in Section 4 the main conclusions are summarized.

2 | THEORETICAL BACKGROUND

2.1 | Confined helium atom: Ground state energy, wave functions and its probability densities

The Hamiltonian of a helium–like atom confined in an impenetrable spherical box of radius r_0 (in the infinite nuclear mass approximation), in atomic units ($\hbar = e = m_e = 1$), is given by

$$\hat{H} = -\frac{1}{2}\nabla_1^2 - \frac{1}{2}\nabla_2^2 + V(\vec{r}_1, \vec{r}_2), \tag{1}$$

where the first two terms on the right-hand side are the electron kinetic energies, and the potential energy is given by:

$$V(\vec{r}_1, \vec{r}_2) = \begin{cases} -\frac{Z}{r_1} - \frac{Z}{r_2} + \frac{1}{r_{12}}, & r_1, r_2 < r_0 \\ \infty, \text{ while} & r_1 \geq r_0 \text{ or } r_2 \geq r_0 \end{cases}, \tag{2}$$

where r_1 is the distance from the nucleus to electron 1, r_2 is the distance from the nucleus to electron 2, $r_{12} = |\vec{r}_1 - \vec{r}_2|$ is the distance from electron 1 to electron 2 and $Z = 2$ is the nuclear charge for the helium atom. Inside the spherical barrier $r_1, r_2 < r_0$, the potential energy is given by the Coulombic attractive interaction between the electrons and the nucleus, and the repulsive interaction between the electrons.

In order to solve the problem of finding the energy eigenvalues it is convinient to define the Hylleraas coordinates: $s \equiv r_1 + r_2$, $t \equiv -r_1 + r_2$ and $u \equiv r_{12}$. The Hamiltonian of the confined helium atom in Hylleraas coordinates can be written as:

$$\begin{aligned}\hat{H} = &-\left(\frac{\partial^2}{\partial s^2}+\frac{\partial^2}{\partial t^2}+\frac{\partial^2}{\partial u^2}\right)-2\frac{s(u^2-t^2)}{u(s^2-t^2)}\frac{\partial^2}{\partial s\partial u}\\ &-2\frac{t(s^2-u^2)}{u(s^2-t^2)}\frac{\partial^2}{\partial t\partial u}-\frac{4s}{(s^2-t^2)}\frac{\partial}{\partial s}+\frac{4t}{(s^2-t^2)}\frac{\partial}{\partial t}\\ &-\frac{2}{u}\frac{\partial}{\partial u}-4Z\frac{s}{s^2-t^2}+\frac{1}{u}.\end{aligned} \tag{3}$$

In this report we only study the ground state of the confined helium atom. To obtain the approximate energy and its corresponding wave function, in terms of the box size r_0, we use the Ritz variational method. We propose two types of trial wave functions: uncorrelated and correlated wave functions.

2.1.1 | Uncorrelated wave function

Within the direct variational method the wave function is constructed as the wave function of the free (unconfined) system multiplied by a cut-off function. The simplest wave function is given by the product of two hydrogen–like wave functions, multiplied by the cut-off function $(r_0 - r_1)(r_0 - r_2)$ that makes the wave function vanish at the confining surface of the spherical cavity. The uncorrelated wave function is:

$$\psi_0 = Be^{-\alpha(r_1+r_2)}(r_0 - r_1)(r_0 - r_2), \tag{4}$$

which in Hylleraas coordinates it can be written as

$$\psi_0(s,t,u) = Be^{-\alpha s}\left(r_0 - \frac{s-t}{2}\right)\left(r_0 - \frac{s+t}{2}\right), \tag{5}$$

where α is a variational parameter and B is a normalization constant.

2.1.2 | Wave functions with electronic correlation

We used five wave functions that include electronic correlation u. The trial wave functions in Hylleraas coordinates are the following:

$$\psi_1(s,t,u) = Be^{-\alpha s}(1+\beta u)\chi(s,t,u;r_0), \tag{6}$$

$$\psi_2(s,t,u) = Be^{-\alpha s}(1+\beta u+\gamma t^2)\chi(s,t,u;r_0), \tag{7}$$

$$\psi_3(s,t,u) = Be^{-\alpha s}(1+\beta u+\gamma t^2+\delta s^2)\chi(s,t,u;r_0), \tag{8}$$

$$\psi_k(s,t,u) = B\sum_{n,m,\ell} C_{nlm}e^{-\alpha s}s^n t^m u^\ell \chi(s,t,u;r_0), \tag{9}$$

where $k=4$ denotes a seven-term wave function while $k=5$ denotes a 70-term wave function and $n+m+l \le 2,7$, respectively, $\chi(s,t,u;r_0) = \left(r_0 - \frac{s-t}{2}\right)\left(r_0 - \frac{s+t}{2}\right)$ is the cut-off function, and $\alpha, \beta, \gamma, \delta$ and C_{nlm} are variational parameters.

2.1.3 | Energy calculations

As we mentioned above we use the Ritz variational method to obtain the approximate energy and wave functions. In this approach we minimize the energy functional

$$E=\frac{\langle\psi|\hat{H}|\psi\rangle}{\langle\psi|\psi\rangle}, \tag{10}$$

with respect to the variational parameters, where $\hat{H}$ is the Hamiltonian in Hylleraas coordinates (Equation 3) and $\psi=\psi_i, i=0,\ldots,5$.

For the confined helium atom, different expressions [19, 35, 86] have been used to evaluate the integrals involved in the energy functional; those expressions are equivalent and provide the same results. The expression that we used to evaluate the integrals in the energy functional is the following [86]:

$$\begin{aligned}\int f d\tau &= 2\pi^2\int_0^{r_0} ds\int_0^{s} dt\int_t^{s} f(s,t,u)(s^2-t^2)u\,du,\\ &+2\pi^2\int_{r_0}^{2r_0} ds\int_0^{2r_0-s} dt\int_t^{s} f(s,t,u)(s^2-t^2)u\,du,\end{aligned} \tag{11}$$

where f can be either $\hat{H}$ or the probability density $|\psi|^2$.

All the integrals involved in the calculation of the energy functional E (Equation 10) are obtained in analytical form using Mathematica and/or Maple programs. The minimization of the energy functional is performed using the function minimization commands of each program, in this way we obtain the minimum energy and the set of optimal variational parameters of the wave functions. The minimum energy for each wave function is shown in Table 1, as well as graphically in the Figure 1.

2.1.4 | Quantum probability density

The one–electron probability density is obtained by integrating over the coordinates of the other electron. The probability density associated with the wave function ψ_0 is given by

$$\rho_0(\vec{r})=Be^{-2\alpha r} \tag{12}$$

whereas for the wave functions $\psi_1,\ldots,\psi_5$ the probability density is obtained by [87]:

$$\begin{aligned}\rho_i(\vec{r}) &= \frac{2\pi}{r}\left\{\int_0^{r} dr_2 r_2\int_{r-r_2}^{r+r_2} dr_{12} r_{12}\psi(r,r_2,r_{12})^2\right.\\ &\left.+\int_r^{r_0} dr_2 r_2\int_{r_2-r}^{r_2+r} dr_{12} r_{12}\psi(r,r_2,r_{12})^2\right\}, i=1,\ldots,5,\end{aligned} \tag{13}$$

where $\psi(r,r_2,r_{12})$ is given by Equations (6), (7), (8), or (9) respectively.

TABLE 1 The ground state energy for uncorrelated and correlated wave functions as a function of confinement radius r_0.

r_0(a.u.)	$E(\psi_0)$	$E(\psi_1)$	$E(\psi_2)$	$E(\psi_3)$	$E(\psi_4)$	$E(\psi_5)$
.5000	22.9229	22.9043	22.8321	22.7765	22.7426	22.7413
.6000	13.4250	13.3986	13.3645	13.3421	13.3204	13.3181
.7000	7.9968	7.9642	7.9490	7.9382	7.9278	7.9252
.8000	4.6656	4.6282	4.6224	4.6201	4.6120	4.6104
.9000	2.5117	2.4706	2.4691	2.4706	2.4642	2.4632
1.0000	1.0625	1.0186	1.0185	1.0214	1.0163	1.0157
2.0000	−2.5284	−2.5797	−2.5976	−2.5994	−2.5977	−2.6040
3.0000	−2.7935	−2.8419	−2.8651	−2.8659	−2.8679	−2.8724
4.0000	−2.8301	−2.8763	−2.8955	−2.8960	−2.8981	−2.9004
5.0000	−2.8391	−2.8843	−2.9003	−2.9007	−2.9023	−2.9034
6.0000	−2.8425	−2.8871	−2.9015	−2.9018	−2.9029	−2.9036
10.0000	−2.8462	−2.8900	−2.9022	−2.9026	−2.9033	−2.9037
∞	−2.84766	−2.8911	−2.9024	−2.9027	−2.9034	−2.9037

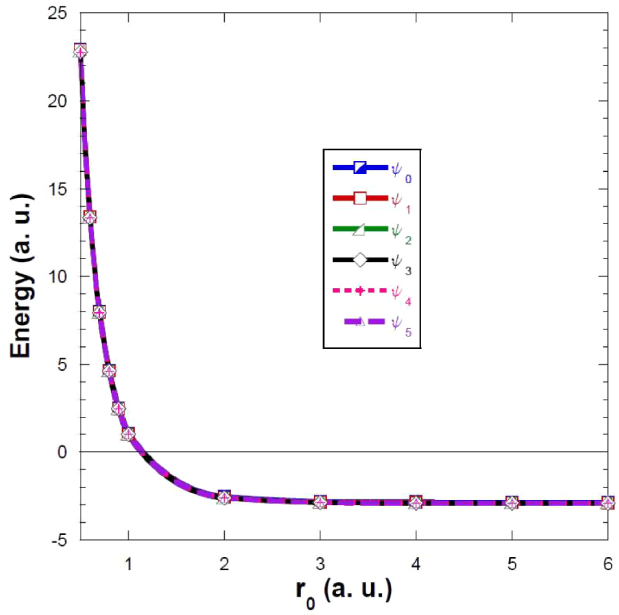

FIGURE 1 Energy variation for the helium atom with and without electronic correlation, varying the confinement radius r_0.

The one electron probability density is normalized to unity as

$$\int \rho_i(\vec{r}) d\vec{r} = 1. \tag{14}$$

2.2 | Information-theoretic approach

2.2.1 | Shannon entropy

The Shannon entropy [48, 67, 88–90] is a functional of the probability density $\rho(\vec{r})$ defined by:

$$S_r = -\int \rho(\vec{r}) \ln \rho(\vec{r}) \mathrm{d}\vec{r}. \tag{15}$$

It quantifies the total extent of the density. It has also been used as a measure of localization-delocalization of the electron. A smaller value of S corresponds to a more concentrated distribution, that is, the particle (electron) is more localized.

2.2.2 | Kullback–Leibler entropy

The Kullback–Leibler entropy [79, 89, 91, 92] for a continuous probability distribution $\rho(\vec{r})$, relative to a reference distribution $\rho_{ref}(\vec{r})$ is defined as follows:

$$KL(\rho,\rho_{ref}) = \int \rho(\vec{r}) \ln \frac{\rho(\vec{r})}{\rho_{ref}(\vec{r})} \mathrm{d}\vec{r}, \tag{16}$$

where

$$\int \rho(\vec{r}) \mathrm{d}\vec{r} = \int \rho_{ref}(\vec{r}) \mathrm{d}\vec{r} = 1, \tag{17}$$

verifying $KL(\rho,\rho_{ref}) \geq 0$. It can be seen that $\rho(\vec{r}) = \rho_{ref}(\vec{r}) \Leftrightarrow KL(\rho,\rho_{ref}) = 0$.

2.2.3 | Disequilibrium

Similarly the disequilibrium [85, 93, 94] gives a measure between two distributions, only in this case the deviation is with respect to the equi-probability, also known as equilibrium state. It is determined as follows:

$$D = \int \rho^2(\vec{r})\mathrm{d}\vec{r}. \tag{18}$$

2.2.4 | Tsallis entropy

The Tsallis entropy for the confined helium atom is studied using a wave function with electronic correlation in order to obtain a measure of the correlation intensity. The Tsallis entropy [65, 75, 95–99] is defined as follows:

$$S_q \equiv \frac{1}{q-1}\left(1 - \int \rho^q(\vec{r})\mathrm{d}\vec{r}\right). \tag{19}$$

The Tsallis index q plays a crucial role in identifying the magnitude of correlations in a system. In the limit $q \to 1$, $S_q \to S_r$, that is, the Shannon entropy is recovered.

2.2.5 | Fisher–Shannon complexity

Fisher–Shannon complexity measure for a probability density ρ is defined jointly by the Fisher information $F_r[\rho]$ and the Shannon entropic power. The Fisher information [49, 51–53, 55, 83, 88, 93, 100, 101] is a point-to-point measure of the electron cloud distribution since it is a gradient functional of $\rho(\vec{r})$ and in configuration space is tightly connected to the kinetic energy due to its dependence on the gradient of the distribution. It is interpreted as a measure of the tendency toward disorder, meaning that the larger this quantity is, the more ordered the distribution will be. It is defined by:

$$F_r[\rho] = \int \frac{|\vec{\nabla}\rho(\vec{r})|^2}{\rho(\vec{r})}\mathrm{d}\vec{r}. \tag{20}$$

The entropic Shannon power [94] guarantees the positivity of this quantity and is defined as follows:

$$J[\rho] = \frac{1}{2\pi e}e^{2S[\rho]/3}. \tag{21}$$

It is common to define Fisher–Shannon complexity [53, 83, 84] as follows:

$$C_{FS}[\rho] = F_r[\rho] \times J[\rho] = \frac{1}{2\pi e}F[\rho]e^{2S[\rho]/3}. \tag{22}$$

As a consequence of Stam's inequality [102] this quantity satisfies the following inequality

$$\frac{1}{3}C_{FS}[\rho] \geq 1 \tag{23}$$

for any continuously differentiable probability density ρ. Moreover, this complexity measure is invariant under scaling transformations and translations, and is a monotone measure [103].

3 | RESULTS AND DISCUSSION

3.1 | Shannon entropy

From Table 2 and Figure 2, we can see that in the confinement regime $r_0 > 1$ a.u. the value of the Shannon entropy for the uncorrelated density $S(\rho_0)$ is smaller than the value of the entropies $S(\rho_i)$, $\{i = 1,2,3,4,5\}$, corresponding to the functions including electronic correlation.

Gadre et al. [81] and Hô et al. [104] used the Shannon entropy as a measure of the quality of the basis set of a free molecular system. They constructed a wave function as an expansion in a certain basis, observing that increasing the number of basis functions resulted in a better wave function, and that the Shannon entropy increased as the quality of the wave function improved. Extending Gadre's conjecture to the wave functions used in this work, we conclude that by increasing the number of Hylleraas functions the quality of the wave function improves, that is, it approaches the exact wave function.

From Figure 3, we can observe that the Shannon entropy values calculated with the electronically correlated wave functions are higher than the Shannon entropy of the uncorrelated wave function. The more correlation the wave function contains the higher the value of the Shannon entropy. This is more evident for r_0 greater than 2 a.u. Romera and Dehesa [83] point out that this is because electronic correlation produces a dispersion of the electronic cloud, and therefore, the Shannon entropy increases.

An entirely different situation occurs in the strong confinement regime where $r_0 < 1$ a.u. The value of the Shannon entropy for the uncorrelated wave function $S(\rho_0)$ is smaller than $S(\rho_1)$, the Shannon entropy associated with ψ_1, but is larger than the entropy values for the other correlated wave functions. If Gadre's conjecture could be applied to this situation we would conclude that the best wave function, of those used

TABLE 2 Shannon entropy for different probability densities as a function of the confining radius r_0, and its comparison with those reported by Sen [105].

r_0(a.u.)	$S(\rho_0)$	$S(\rho_1)$	$S(\rho_2)$	$S(\rho_3)$	$S(\rho_4)$	$S(\rho_5)$	[105]
.5000	−1.5142	−1.5129	−1.5181	−1.5181	−1.5257	−1.5247	
.6000	−.9986	−.9967	−1.0012	−1.0065	−1.0083	−1.0068	
.7000	−.5696	−.5670	−.5708	−.5747	−.5767	−.5752	
.8000	−.2046	−.2013	−.2041	−.2066	−.2086	−.2075	
.9000	.1109	.1148	.1131	.1123	.1095	.1108	.1515
1.0000	.3867	.3914	.3910	.3919	.3874	.3898	
2.0000	1.9117	1.9263	1.9587	1.9627	1.9548	1.9735	2.0097
3.0000	2.3673	2.3902	2.4777	2.4803	2.4839	2.5124	2.5241
4.0000	2.4906	2.5161	2.6229	2.6243	2.6381	2.6654	2.6197
5.0000	2.5310	2.5571	2.6628	2.6642	2.6798	2.6986	2.6651
6.0000	2.5481	2.5743	2.6768	2.6783	2.6883	2.7042	2.7042
10.0000	2.5673	2.5937	2.6900	2.6919	2.7029	2.7050	2.7106
∞	2.5749	2.60159	2.6945	2.6967	2.7035	2.7051	2.7117

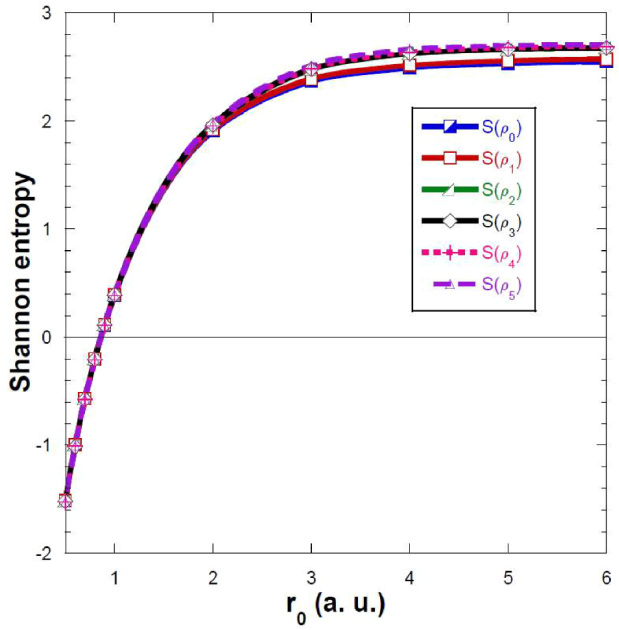

FIGURE 2 Shannon entropy for the helium atom confined in a spherical impenetrable cavity with and without electronic correlation. The values $S(\rho_i)$ are given in Table 2, where $i = 0, 1, 2, 3, 4$, and 5.

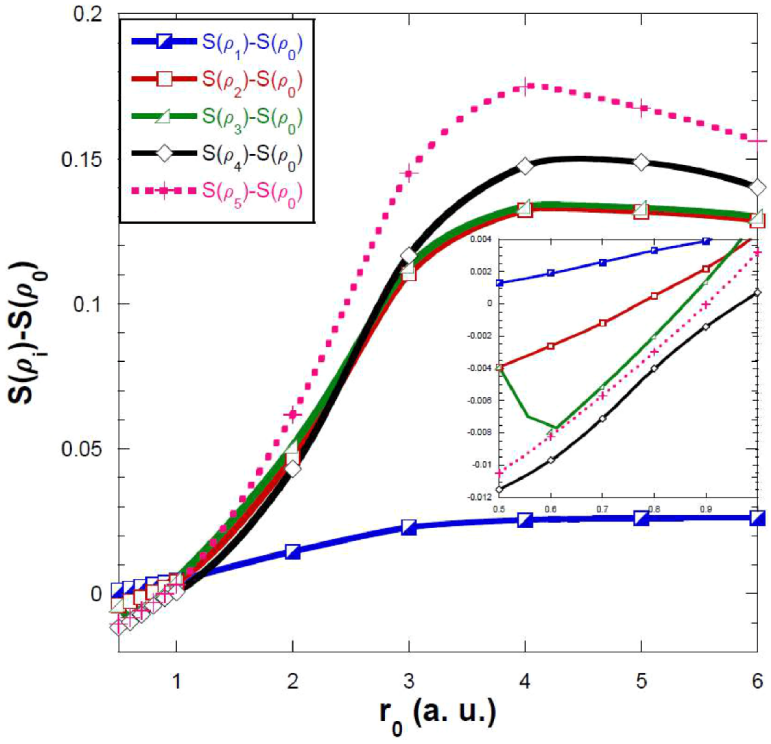

FIGURE 3 Shannon entropy difference $S(\rho_i) - S(\rho_0)$, where $i = 1,2,3,4$, and 5.

in this report, would be ψ_1, and we could state that electronic correlation produces a spread in the electronic probability density. We should mention that our calculations of the Shannon entropy, using the ψ_1 function, are in complete agreement with previously published results [35]. The other wave functions, with higher correlation content, would make the electron density more compact, contrary to what is expected. It has been shown [28, 30] that in the strong confinement regime the electron kinetic energy is so large that the problem can be reasonably well treated by perturbation theory using uncorrelated wave functions, that is, the electron correlation is not so important in this regime. Therefore, a good description of the wave function is obtained by the ψ_1 function.

3.2 | Fisher information

Fisher information is a measure of the concentration of the probability density. Fisher information is a local measure, which is very sensitive to variations of the probability density, even in small regions. However, contrary to Shannon entropy, Fisher information decreases as r_0 increases, as shown in Figure 4, indicating greater delocalization as r_0 increases. The values of Fisher information as a function of r_0, for the different wave functions, with and without correlation, are very similar.

In the region $r_0 > 1$ a.u., the Fisher information values for the correlated wave functions are larger than the corresponding value of the Fisher information for the uncorrelated wave function. In the strong confinement regime $r_0 < 1$ a.u., the Fisher information corresponding to the uncorrelated wave function $F(\rho_0)$ is smaller than $F(\rho_1)$. However, $F(\rho_0)$ is larger than the Fisher information for the ψ_2, ψ_3, ψ_4 and ψ_5 wave functions, which contain more electron correlation than ψ_1. This behavior is most evident from Figure 5 where the difference between the Fisher information for the correlated functions and the Fisher information for the uncorrelated wave function is shown. This difference between these values is entirely due to electronic correlation. It can be seen from the graph that there is a well defined maximum value around $r_0 = 2$ a.u., for the Fisher curves with higher correlation.

3.3 | Kullback–Leibler entropy

The Kullback–Leibler (KL) entropy is a measure of the information that quantifies the amount of information by which the probability density $\rho(\vec{r})$ differs from the reference density $\rho_0(\vec{r})$. This measure is zero when the probability density $\rho(\vec{r})$ is identical to the reference probability density $\rho_0(\vec{r})$. In other words, this measure quantifies the similarity between the two probability densities. When the KL entropy is small the probability densities $\rho(\vec{r})$ and $\rho_0(\vec{r})$ are similar, and when the KL entropy is large, the two probability densities are remarkably different. Figure 6 shows

the KL entropy values for the electronically correlated $\rho_i(\vec{r})$ densities with respect to the uncorrelated $\rho_0(\vec{r})$ reference density. Those values are entirely due to the electronic correlation.

For values of $r_0 > 1$ a.u., the KL entropy values increase with r_0, but even so the densities $\rho_1(\vec{r})$ and $\rho_0(\vec{r})$ remain very similar. The KL entropies for the densities with greater correlation increase with r_0, and have a maximum value near $r_0 = 4$ a.u., and then decrease and tend asymptotically to the values of the free case. The Kullback–Leibler entropy varies with r_0 and its highest value is found around $r_0 = 4$ a.u.

For $r_0 < 1$ a.u., the KL entropies for $\rho_i(\vec{r})$, $i = 2-5$, decrease as r_0 decreases, reach a minimum value and increase again, indicating that the correlation decreases with r_0, KL reaches a minimum value at $r_0 = 1$ a.u. and increases again.

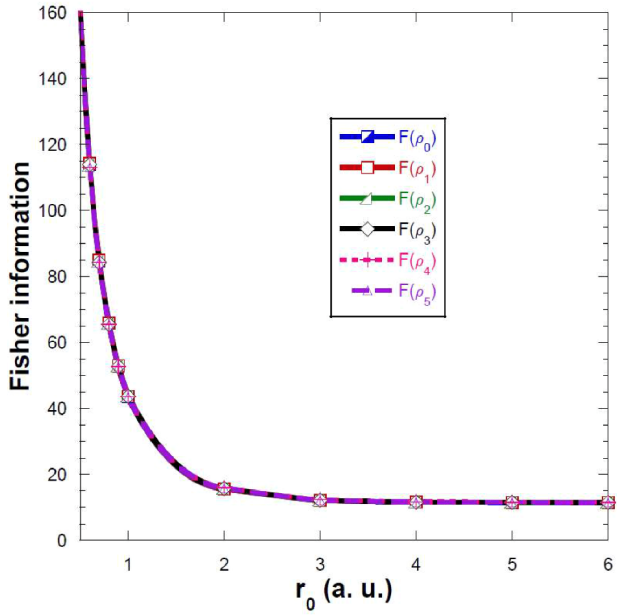

FIGURE 4 Fisher information for the helium atom confined in a spherical impenetrable cavity with and without electronic correlation.

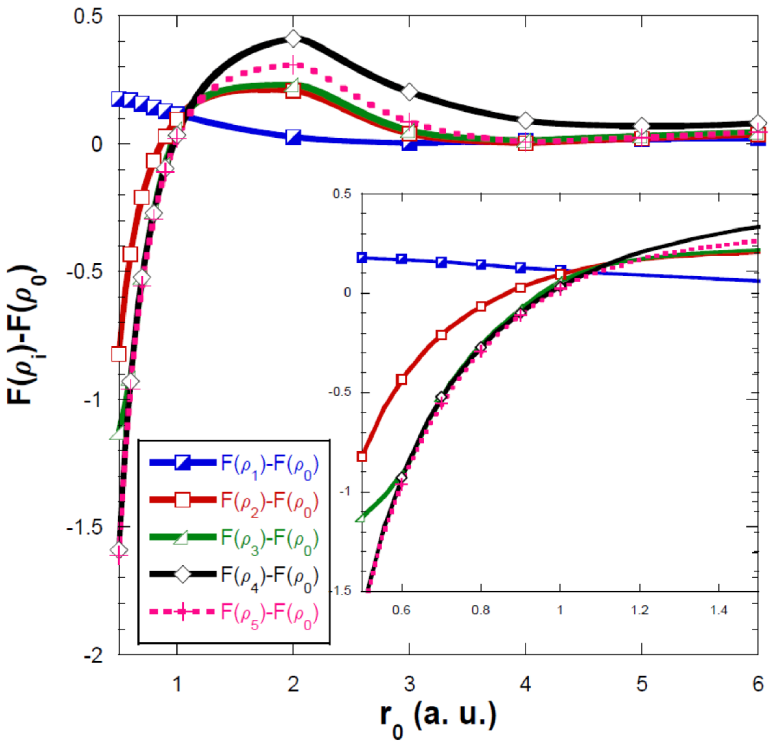

FIGURE 5 Fisher information difference $F(\rho_i) - F(\rho_0)$, where $i = 1,2,3,4$, and 5.

3.4 | Disequilibrium

As can be seen from Figure 7, in the region $0 < r_0 < 2$ the Disequilibrium is a decreasing function of r_0 and it has practically the same value for all wave functions. However, in the region $r_0 > 2$ a separation is shown between the Disequilibrium corresponding to the uncorrelated wave function and those with explicitly correlation terms. As we seen in other entropic measures, the value of the Disequilibrium for the correlated functions is higher than that of the uncorrelated function.

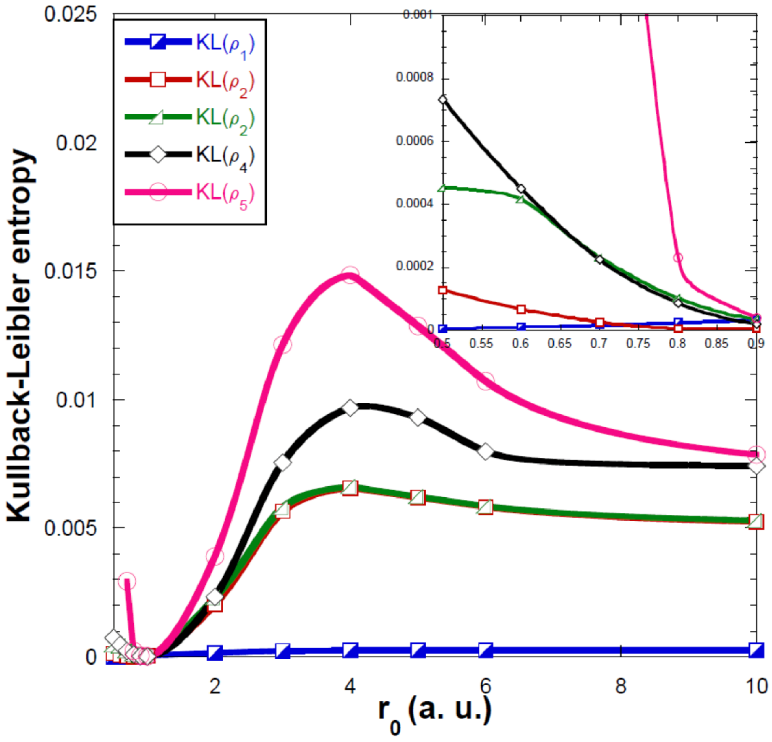

FIGURE 6 Kullback–Leibler entropy for the helium atom confined in a spherical impenetrable cavity.

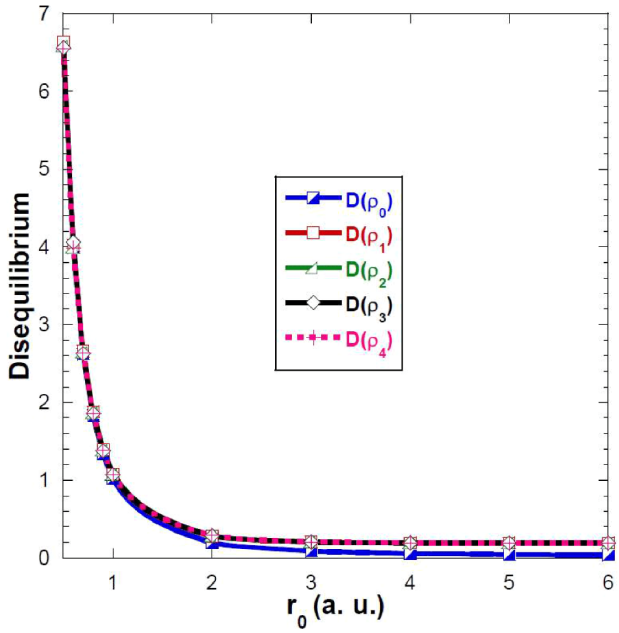

FIGURE 7 Disequilibrium for the helium atom confined in a spherical impenetrable cavity.

3.5 | Tsallis entropy

The Tsallis entropy with a q value different from 1 has been used as a measure of the electronic correlation [75]. Figure 8 shows the Tsallis entropy using a wave function without electronic correlation, where values of $q = .5, ..., .9$ were used. It should be noted that this plot does not provide correlation information. The Tsallis entropy curves have a maximum around .6 a.u. and this becomes more pronounced as q approaches 1. We must remember that in the limiting case $q \to 1$, Tsallis entropy becomes the Shannon entropy, shown in Figures 2 and 3.

The analysis shown below is for $\rho_3(\vec{r})$, however, the behavior of Tsallis entropy for $\rho_i(\vec{r})$, ($i = 1,2,4$, and 5) is very similar. On the other hand, Figure 9 shows the Tsallis entropy with electronic correlation for the same values of q. Here we can notice that as the confinement radius becomes smaller the correlation decreases, as expected, since the kinetic energy is greater than the potential energy in the region of strong confinement. In addition, we notice that the correlation is greater for $q = .5$ and as we increase the value of q the correlation decreases. Finally, in

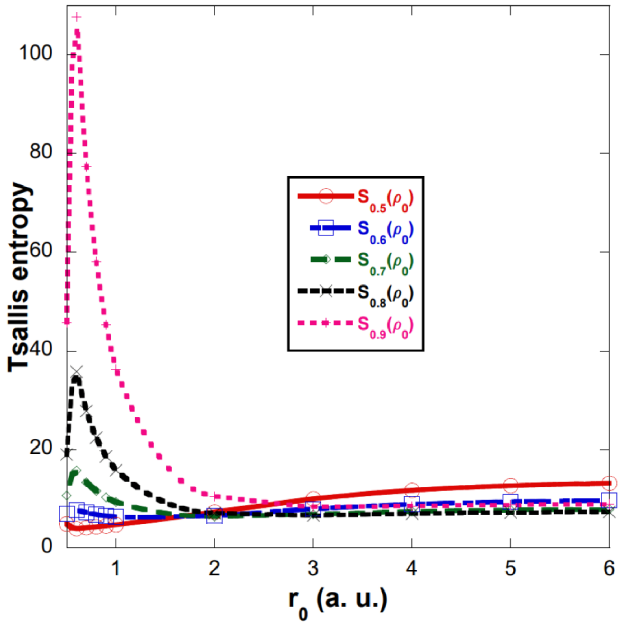

FIGURE 8 Tsallis entropy for the helium atom confined in a spherical impenetrable cavity without electronic correlation.

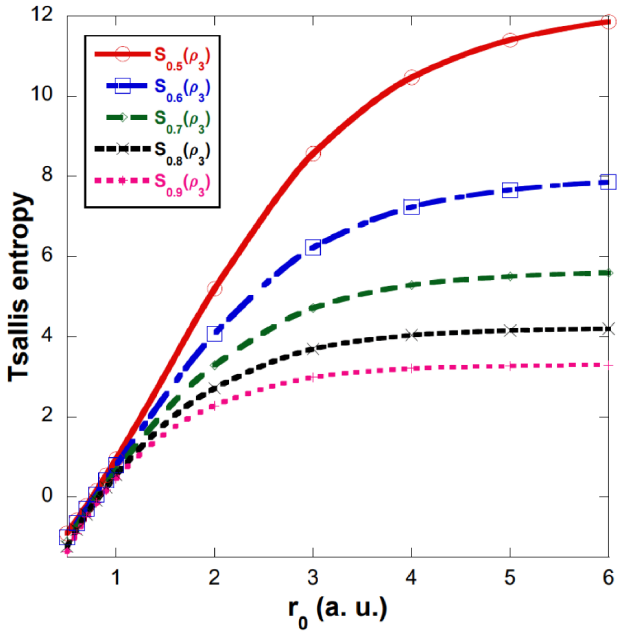

FIGURE 9 Tsallis entropy for the helium atom confined in a spherical impenetrable cavity with electronic correlation for $S_q(\rho_3)$.

Figure 10 we plot the difference: Tsallis entropy with correlation–Tsallis entropy without correlation. The difference $S_q(\rho_3) - S_q(\rho_0)$ is due completely to the correlation.

3.6 | Fisher–Shannon complexity

The Fisher–Shannon complexity is a measure of the probability density distribution in a global-local form that has been used as a measure of the correlation energy by Dehesa et al. [83]. This interpretation makes sense if we look at Figure 11, in which we notice that around $r_0 = 1.5$ a.u. there

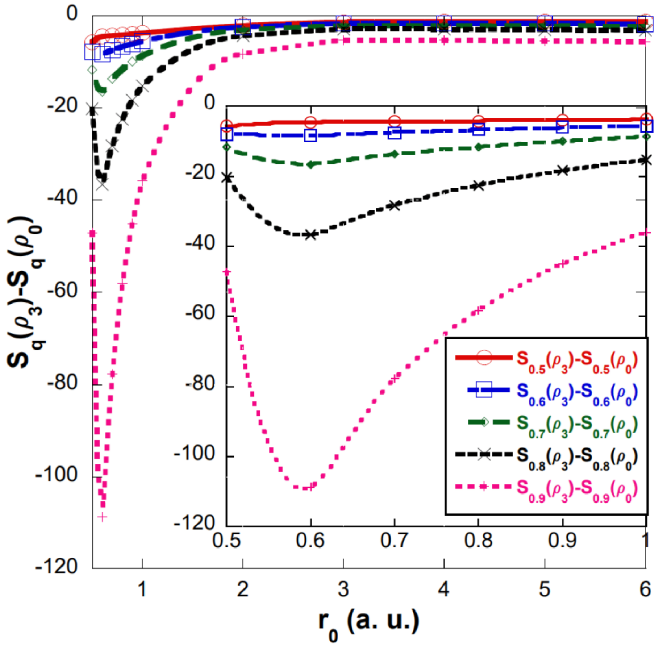

FIGURE 10 Tsallis entropy difference $S_q(\rho_3) - S_q(\rho_0)$.

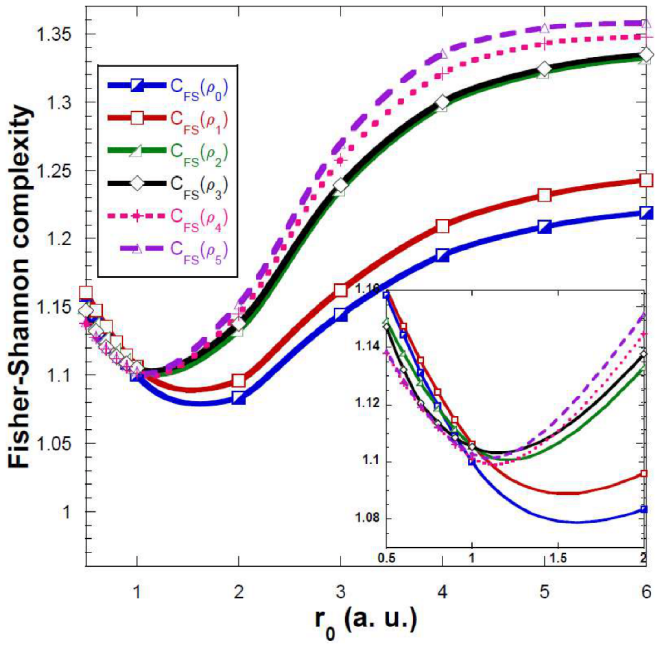

FIGURE 11 Fisher–Shannon complexity for the helium atom confined in a spherical impenetrable cavity with and without electronic correlation.

is a minimum, which is close to the value of $r_0 = 2$ a.u., at which the maximum of the correlation energy was found by Wilson et al. [31]. For values of $r_0 < 1$ a.u. the values of all curves are very similar. For $r_0 > 1$ a.u. the Fisher–Shannon complexities for the correlated wave functions are all higher than for the uncorrelated wave function.

4 | CONCLUSIONS

In this work, we obtained the energies and wave functions of the helium atom confined in a spherical box with impenetrable walls. We used the variational method and as trial wave functions we employed one function without electronic correlation (ψ_0, Equation 4) and five functions with different degree of correlation (Equations 5–9), where the trialfunction ψ_5 gives accurate energy values and quality wave functions. We constructed the probability densities of the five trial functions and calculated the Shannon entropy, Fisher information, Kullback–Leibler entropy, Tsallis entropy and Fisher–Shannon complexity as a function of the radius of the spherical box r_0.

The main conclusions derived from the present work are summarized as follows:

- Each of the diverse information-theoretic functionals here considered reveals, in different ways, a specific dependence of their respective values in terms of the confinement radius r_0. Most usually, the corresponding curves display structured behaviors accordingly with a diversity of ranges for r_0.
- Nevertheless, the visualizations just mentioned for a given functional are nuanced, to a greater or lesser extent, by considering the whole set of wavefunctions to describe the confined system. The comparative analysis emphasizes the relevance of interelectronic correlation, as revealed by the information-theoretic values. This comment applies both to the structure and ordering of curves.
- For all information measures, except Tsallis entropy, the difference between the values obtained with a wave function with correlation ψ_i, ($i = 1 - 5$) and with the uncorrelated function ψ_0, is entirely due to electronic correlation, then, we may consider this difference as a measure of correlation. All information measures show evidence of electronic correlation. The electronic correlation is not constant but varies with r_0. The maximum value of the information theoretic correlation measure varies with the type of information measure used.

The above major conclusions are detailed below for the information measures considered, attending to the different functionals and their features:

- Maxima and minima: For example, for Shannon entropy the maximum value is reached around $r_0 = 4$ a.u., while for Fisher information at $r_0 = 2$ a.u., for Kullback–Leibler entropy at $r_0 = 4$ a.u., while for the Tsallis entropy a minimum is observed around $r_0 = .6$ a.u., and for the Fisher–Shannon complexity the minimum is located around $r_0 = 1.6$ a.u., which is close to the point $r_0 = 2$ a.u., at which Wilson et al. [31] find a higher correlation energy.
- Shannon entropy: To understand the behavior of the Shannon entropy associated with the trial functions $\psi_0,...,\psi_5$ as a function of r_0, it was convenient to divide the variable r_0 into two regions. In the first region $r_0 > 1$, the Shannon entropy increases when employing a wave function with a larger number of correlation terms, this is the usual behavior in free atoms [81]. While in the second region $r_0 < 1$ the Shannon entropy for wave functions $\psi_2,...,\psi_5$ has an opposite behavior to the one presented in the region $r_0 > 1$. However, the Shannon entropy for ψ_1 is always higher than for ψ_0 (Figure 3). The Shannon entropy and correlation energy show a similar trend at $.5 < r_0 < 2$, this becomes different at $2 < r_0 < 4.5$, and for $r_0 > 4.5$ both quantities have an almost constant behavior. In the region $.5 < r_0 < 2$, we see that as r_0 decreases the Shannon entropy decreases (localization) and also the correlation energy decreases.
- The Fisher information of the five wave functions as a function of the confining radius r_0 is a rapidly decreasing function. In the region $.5 < r_0 < 2$ the Fisher information increases (localization) and the correlation energy decreases, as r_0 decreases, in agreement with the Shannon entropy results.
- The Kullback–Leibler entropy indicates that for values of $r_0 < 1$, the probability densities $\rho_1,...,\rho_5$, or their respective wave functions, are similar to the uncorrelated density ρ_0, or its corresponding wave function ψ_0. In that region the KL entropy is small, the wave functions are very similar but the correlation energy is different from zero. At $r_0 = 2$ the values of the entropies split lightly, but at that point the correlation energy has a maximum. The maximum of the KL entropy is reached near $r_0 = 4$ but at that value of r_0 the correlation energy is already almost a constant. In this study the KL entropy is useful to establish the similarity between two wave functions but not to describe the correlation energy.
- The Disequilibrium is a decreasing function of r_0. The values of Disequilibrium are almost the same for $0 < r_0 < 2$. In the region $r_0 > 2$ the values of Disequilibrium for the correlated functions overlap, in this region the Disequilibrium value for the functions with correlation is higher than for the function without correlation.
- The Fisher–Shannon complexity and the correlation energy show almost opposite behaviors, near the position where the Fisher–Shannon complexity has a minimum the correlation energy has its maximum value. We can say that when the FSC decreases the correlation energy increases and vice versa.

Finally, let us mention the information-theoretic study in terms of correlation energy, as provided in the Appendix. Although it remains as an open problem, important conclusions are already derived from the results included here. Attention is paid to the comparative analysis among the correlation energy and each of the information measures.

ACKNOWLEDGMENTS

N. A. and C. E. would like to thank R. P. Sagar for his comments on an early version of this work. CONACyT and Universidad Autónoma Metropolitana (Mexico) is gratefully acknowledged for providing a scholarship for doctoral studies (C. E.) and financial support by *Sistema Nacional de Investigadores*(NA). J. C. A. belongs to the research group FQM-207, and gratefully acknowledges financial support by the Spanish projects PID2020-113390GB-I00 (MICIN), PY20-00082 (ERDF-Junta de Andalucía), and A-FQM-52-UGR20 (ERDF-University of Granada). We thanks to the anonymous referees for their comments.

ORCID

N. Aquino https://orcid.org/0000-0002-3795-0304

REFERENCES

[1] F. M. Fernández, E. A. Castro, *Kinam* **1982**, *4*, 193.
[2] P. O. Fröman, S. Yngve, N. Fröman, *J. Math. Phys.* **1987**, *28*, 1813.
[3] W. Jaskólski, *Phys. Rep.* **1996**, *271*, 1.
[4] A. L. Buchachenko, *J. Phys. Chem. B* **2001**, *105*, 5839.
[5] J. P. Connerade, V. K. Dolmatov, P. A. Lakshmi, *J. Phys. B: At., Mol. Opt. Phys.* **2000**, *33*, 251.
[6] J. R. Sabin, E. Brändas, S. A. Cruz Eds., *Theory of Confined Quantum Systems*. Parts I and II, Academic Press, Cambridge **2009**.
[7] K. D. Sen, V. I. Pupyshev, H. E. Montgomery Jr., *Adv. Quantum Chem.* **2009**, *57*, 25.
[8] K. D. Sen Ed., *Electronic structure of quantum confined atoms and molecules*, Springer, Switzerland **2014**.
[9] E. Ley-Koo, *Rev. Méx. Fis.* **2018**, *64*, 326.
[10] S. W. Koch, *Semiconductor Quantum Dots*, Vol. 2, World Scientific, New Jersey **1993**.
[11] P. Harrison, A. Valavanis, *Quantum Wells, Wires and Dots: Theoretical and Computational Physics of Semiconductor Nanostructures*, John Wiley & Sons, New Jersey **2016**.
[12] A. Michels, J. De Boer, A. Bijl, *Physica* **1937**, *4*, 981.
[13] E. Ley-Koo, S. Rubinstein, *J. Chem. Phys.* **1979**, *71*, 351.
[14] J. L. Marin, S. A. Cruz, *J. Phys. B: At., Mol. Opt. Phys.* **1992**, *25*, 4365.
[15] N. Aquino, *Adv. Quantum Chem.* **2009**, *57*, 123.
[16] H. E. Montgomery Jr., K. D. Sen, *Phys. Lett. A* **2012**, *376*, 1992.
[17] S. Goldman, C. Joslin, *J. Phys. Chem.* **1992**, *96*, 6021.
[18] A. Solórzano, N. Aquino, A. Flores-Riveros, *Can. J. Phys.* **2016**, *94*, 894.
[19] C. A. Ten Seldam, S. R. De Groot, *Physica* **1952**, *18*, 891.
[20] B. M. Gimarc, *J. Chem. Phys.* **1967**, *47*, 5110.
[21] E. V. Ludeña, *J. Chem. Phys.* **1978**, *69*, 1770.
[22] T. D. Young, R. Vargas, J. Garza, *Phys. Lett. A* **2016**, *380*, 712.
[23] E. V. Ludeña, M. Gregori, *J. Chem. Phys.* **1979**, *71*, 2235.
[24] N. Aquino, J. Garza, A. Flores-Riveros, J. F. Rivas-Silva, K. D. Sen, *J. Chem. Phys.* **2006**, *124*, 054311.
[25] C. Joslin, S. Goldman, *J. Phys. B: At., Mol. Opt. Phys.* **1992**, *25*, 1965.
[26] N. Aquino, A. Flores-Riveros, J. F. Rivas-Silva, *Phys. Lett. A* **2003**, *307*, 326.
[27] A. Flores-Riveros, A. Rodriguez-Contreras, *Phys. Lett. A* **2008**, *372*, 6175.
[28] A. Flores-Riveros, N. Aquino, H. E. Montgomery Jr., *Phys. Lett. A* **2010**, *374*, 1246.
[29] C. Laughlin, S. I. Chu, *J. Phys. A Theor. Mat.h. Phys.* **2009**, *42*, 265004.
[30] H. E. Montgomery Jr., N. Aquino, A. Flores-Riveros, *Phys. Lett. A* **2010**, *374*, 2044.
[31] C. L. Wilson, H. E. Montgomery Jr., K. D. Sen, D. C. Thompson, *Phys. Lett. A* **2010**, *374*, 4415.
[32] N. Aquino, *AIP Conference Proceedings*, Vol. 1579, American Institute of Physics, College Park, USA **2014**, p. 136.
[33] C. Le Sech, A. Banerjee, *J. Phys. B: At., Mol. Opt. Phys.* **2011**, *44*, 105003.
[34] S. Bhattacharyya, J. K. Saha, P. K. Mukherjee, T. K. Mukherjee, *Phys. Scr.* **2013**, *87*, 065305.
[35] W. S. Nascimento, M. M. de Almeida, F. V. Prudente, *Eur. Phys. J. D* **2021**, *75*, 171.
[36] D. Baye, J. Dohet-Eraly, *Phys. Chem. Chem. Phys.* **2015**, *17*, 31417.
[37] S. Ting-yun, B. Cheng-Guang, L. Bai-Wen, *Commun. Theor. Phys.* **2001**, *35*, 195.
[38] S. B. Doma, F. N. El-Gammal, *J. Theor. Appl. Phys.* **2012**, *6*, 1.
[39] A. Sarsa, C. Le-Sech, *J. Chem. Theory Comput.* **2011**, *7*, 2786.
[40] J. Garza, R. Vargas, A. Vela, *Phys. Rev. E* **1998**, *58*, 3949.
[41] S. Majumdar, A. K. Roy, *Quantum Rep.* **2020**, *2*, 189.
[42] S. Majumdar, A. K. Roy, *Int. J. Quantum Chem.* **2021**, *121*, e26630.
[43] H. E. Montgomery Jr., V. I. Pupyshev, *Phys. Lett. A* **2013**, *377*, 2880.
[44] H. E. Montgomery Jr., V. I. Pupyshev, *Theor. Chem. Acc.* **2015**, *134*, 1.
[45] J. K. Saha, S. Bhattacharyya, T. K. Mukherjee, *Int. J. Quantum Chem.* **2016**, *116*, 1802.
[46] Y. Yakar, B. Çakir, A. Özmen, *Int. J. Quantum Chem.* **2011**, *111*, 4139.
[47] V. I. Pupyshev, H. E. Montgomery Jr., *Theor. Chem. Acc.* **2017**, *136*, 1.
[48] C. E. Shannon, *Bell Syst. Tech. J.* **1948**, *27*, 379.
[49] R. A. Fisher, *Proc. Camb. Phil. Soc.* **1925**, *22*, 700.
[50] M. A. Nilsen, I. L. Chuang, *Quantum Computation and Quantum Information*, Cambridge University Press, Cambridge **2005**.

[51] S. López-Rosa, R. O. Esquivel, J. C. Angulo, J. Antolín, J. S. Dehesa, N. Flores-Gallegos, *J. Chem. Theory Comput.* **2010**, *6*, 145.
[52] R. González-Férez, J. Dehesa, *Eur. Phys. J D-Atomic, Molecular, Optic. Plasma Phys.* **2005**, *32*, 39.
[53] J. C. Angulo, J. Antolín, K. D. Sen, *Phys. Lett. A* **2008**, *372*, 670.
[54] C. P. Panos, K. D. Sen, in *Statistical complexity, Application in electronic structure, Chapter 3* (Ed: K. D. Sen), Springer, New York **2011**.
[55] R. F. Nalewajski, *Information Theory of Molecular Systems*, Elsevier Science, Amsterdam **2006**.
[56] P. Ziesche, *Int. J. Quantum Chem.* **1995**, *56*, 363.
[57] D. M. Collins, *Z Naturforschung A* **1993**, *48*, 68.
[58] Y. Wang, P. Knowles, J. Wang, *Phys. Rev. A* **2021**, *103*, 062808.
[59] B. R. Frieden, *Physics from Fisher information: a unification*, Cambridge University Press, Cambridge **1998**.
[60] R. Stoica, J. Zerubia, J. M. Francos, *Proc.IEEE Intl. Conf. Image Process*, IEEE, Kuala Lumpur **1998**, p. 794.
[61] M. Prato, L. Zanni, *J. Phys. Conf. Ser. J. Phys* **2008**, 012085.
[62] R. Silva, G. S. Franca, C. S. Vilar, J. S. Alcaniz, *Phys. Rev. E* **2006**, *73*, 026102.
[63] M. Bertero, M. Piana, *inverse problem in biomedical Imaging: Modeling and Methods of Solution*, Springer-Verlag, Italy **2006**.
[64] H. A. Ben, *J. Electron. Image.* **2006**, *15*, 013011.
[65] A. F. Martins, P. M. Aguiar, M. A. Figueiredo, *2008 IEEE Information Theory Workshop*, IEEE, Portugal **2008**, p. 298.
[66] A. F. Martins, N. A. Smith, E. P. Xing, P. M. Aguiar, M. A. Figueiredo, *J. Mach. Learn. Res.* **2009**, *10*, 935.
[67] S. J. C. Salazar, H. G. Laguna, B. Dahiya, V. Prasad, R. P. Sagar, *Eur. Phys. J. D* **2021**, *75*, 127.
[68] H. G. Laguna, S. J. Salazar, R. P. Sagar, *J. Math. Chem.* **2022**, *60*, 1422.
[69] S. J. Salazar, H. G. Laguna, R. P. Sagar, *EPJ. Plus* **2022**, *137*, 1.
[70] S. J. Salazar, H. G. Laguna, R. P. Sagar, *Phys. Rev. A* **2023**, *107*, 042417.
[71] C. Martínez-Flores, M. A. Martínez-Sánchez, R. Vargas, J. Garza, *Eur. Phys. J. D* **2021**, *75*, 1.
[72] R. J. Yáñez, W. V. Assche, J. S. Dehesa, *Phys. Rev. A* **1994**, *50*, 3065.
[73] K. D. Sen, C. P. Panos, K. C. Chatzisavvas, C. C. Moustakidis, *Phys. Lett. A* **2007**, *364*, 286.
[74] N. Aquino, A. Flores-Riveros, J. F. Rivas-Silva, *Phys. Lett. A* **2013**, *377*, 2062.
[75] I. Nasser, C. Martinez-Flores, M. Zeama, R. Vargas, J. Garza, *Phys. Lett. A* **2021**, *392*, 127136.
[76] D. C. Thompson, J. S. Anderson, K. Sen, *Int. J. Quantum Chem.* **2021**, *121*, e26549.
[77] K. D. Sen Ed., *Statistical complexity: applications in electronic structure*, Springer Science & Business Media, Berlin **2011**.
[78] M. Ho, V. H. Smith Jr., D. F. Weaver, C. Gatti, R. P. Sagar, R. O. Esquivel, *J. Chem. Phys.* **1998**, *108*, 5469.
[79] M. Ho, D. F. Weaver, V. H. Smith Jr., R. P. Sagar, R. O. Esquivel, *Phys. Rev. A* **1998**, *57*, 4512.
[80] S. R. Gadre, *Phys. Rev. A* **1984**, *30*, 620.
[81] S. R. Gadre, S. B. Sears, S. J. Chakravorty, R. D. Bendale, *Phys. Rev. A* **1985**, *32*, 2602.
[82] S. R. Gadre, R. J. Bendale, A. P. Gejji, *J. Phys. B: At Mol. Phys.* **1985**, *18*, 138.
[83] E. Romera, J. S. Dehesa, *J. Chem. Phys.* **2004**, *120*, 8906.
[84] C. Vignat, J. F. Bercher, *Phys. Lett. A* **2003**, *312*, 27.
[85] R. López-Ruiz, J. Sañudo, E. Romera, X. Calbet, *Statistical complexity and Fisher-Shannon information: Applications*, Applications in Electronic Structure, Statistical Complexity **2011**, p. 65.
[86] X. Y. Pan, V. Sahni, L. Massa, K. D. Sen, *J. Theor. Comput. Chem.* **2011**, *965*, 202.
[87] R. Benesch, *J. Phys. B: At., Mol. Opt. Phys.* **1971**, *4*, 1403.
[88] I. Nasser, A. Abdel-Hady, *Can. J. Phys.* **2020**, *98*, 784.
[89] J. C. Angulo, J. Antolín, S. López-Rosa, R. O. Esquivel, *Phys. A* **2010**, *389*, 899.
[90] P. W. Lamberti, A. P. Majtey, *Phys. A* **2003**, *329*, 81.
[91] S. Kullback, R. A. Leibler, *Ann. Math. Stat.* **1951**, *22*, 79.
[92] A. Majtey, P. W. Lamberti, M. T. Martin, A. Plastino, *Eur. Phys. J D-Atomic, Molecular, Optic. Plasma Phys.* **2005**, *32*, 413.
[93] C. R. Estañón, N. Aquino, D. Puertas-Centeno, J. S. Dehesa, *Int. J. Quantum Chem.* **2020**, *120*, e26192.
[94] R. López Ruiz, J. Sañudo, *J. Comput. Sci.* **2015**, *2*, 100122.
[95] A. Vershynina, *Quantum Inf. Process* **2023**, *22*, 127.
[96] C. Tsallis, *J. Stat. Phys.* **1988**, *52*, 479.
[97] J. Antolín, S. López-Rosa, J. C. Angulo, R. O. Esquivel, *J. Chem. Phys.* **2010**, *132*, 044105.
[98] J. C. Angulo, J. Antolín, S. López-Rosa, R. O. Esquivel, *Phys. A* **2011**, *390*, 769.
[99] C. Tsallis, *J. Comput. Appl. Math.* **2009**, *227*, 51.
[100] M. A. Martínez-Sánchez, C. Martínez-Flores, R. Vargas, J. Garza, R. Cabrera-Trujillo, K. D. Sen, *Phys. Rev. E* **2021**, *103*, 043202.
[101] C. R. Estañón, N. Aquino, D. Puertas-Centeno, J. S. Dehesa, *Int. J. Quantum Chem.* **2021**, *121*, e26424.
[102] A. J. Stam, *Inf. Control.* **1959**, *2*, 101.
[103] Ł. Rudnicki, I. V. Toranzo, P. Sánchez-Moreno, J. S. Dehesa, *Phys. Lett. A* **2016**, *380*, 377.
[104] M. Hô, R. P. Sagar, V. H. Smith Jr., R. O. Esquivel, *J Phys B: Atomic, Molecul. Optic. Phys.* **1994**, *27*, 5149.
[105] K. D. Sen, *J. Chem. Phys.* **2005**, *123*, 074110.

How to cite this article: C. R. Estañón, H. E. Montgomery Jr., J. C. Angulo, N. Aquino, *Int. J. Quantum Chem.* **2024**, *124*(4), e27358.
https://doi.org/10.1002/qua.27358

APPENDIX: CORRELATION ENERGY AND ENTROPIES

The correlation energy E_{corr} is defined by:

$$E_{corr} = E_{exact} - E_{HF} \tag{A1}$$

where E_{exact} are the exact energies, which we will approximate by the energy obtained with the 70-term trial wave function, for each value of r_0, whereas E_{HF} are the energies obtained by the Hartree-Fock method [31]. The correlation energies used in this work are the same reported by Wilson et al. [31].

The Figure A1 shows the informational measures, for the five trial functions, and the correlation energy. In each figure, on the left vertical axis the values of the informational measures are reported, while on the right vertical axis are the values of the correlation energies.

The correlation energy for $r_0 = .5$ has a value close to $-.05$ a.u., its value increases as r_0 grows, until it reaches a maximum value near $r_0 = 2$, then slowly decreases until it reaches a value very close to that of free helium atom at $r_0 = 10$.

Figure A1A shows a coincidence in the increasing trend of Shannon entropy (delocalization) and correlation energy, as a function of r_0, up to a value close to $r_0 = 2$, then, the Shannon entropy curves increase very slowly with r_0 up to about 4.5. For $r_0 > 4.5$ their values remain constant. In the interval $2 < r_0 < 4.5$, E_{corr} and Shannon entropy show different trends. However, for $r_0 > 4$ the Shannon entropy and correlation energy follow the same trend again.

In Figure A1B, it is shown that the Fisher information decreases monotonically with r_0. In the region $0 < r_0 < 2$ Fisher information grows (localization) fast as r_0 decreases, while the correlation energy decreases. As mentioned before, correlation energy has a maximum around $r_0 = 2$, while Fisher information decreases (delocalization) as r_0 increases. For $r_0 > 4.5$, both curves remain constant.

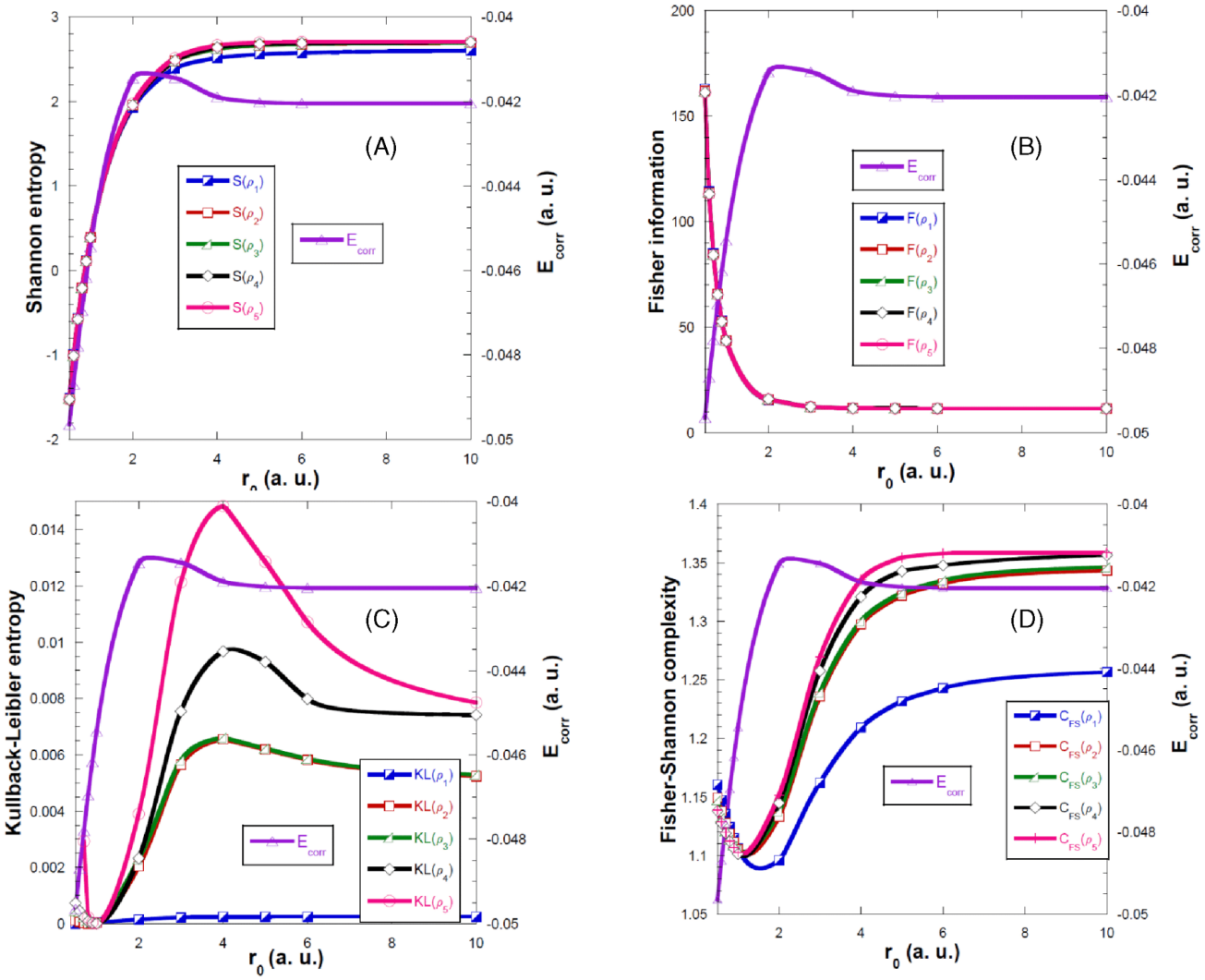

FIGURE A1 Informational measures compared to correlation energy for the helium atom confined in a spherical impenetrable cavity.

Figure A1C shows the Kullback–Leibler entropy and correlation energy curves. In the region $.5 < r_0 < 2$ the Kullback–Leibler entropy curves are concave upward and present a small minimum, close to $r_0 = 1$, a behavior that is not shared by the correlation energy curve. It should be noted that in this region the uncorrelated wave function and the correlated functions are very similar but the correlation energy is different from zero. The Kullback–Leibler entropy curves have their maximum near $r_0 = 4$, while the correlation energy has its maximum near $r_0 = 2$. For values of $r_0 \geq 4.5$, the entropy curves decrease and tend asymptotically to the respective values of the free case, while the correlation energy remains constant.

In Figure A1D, we observe opposite behaviors of the curves of the Fisher Shannon complexities and the correlation energy curve. The curves of the F–S complexities have a minimum at a point in the interval $1 < r_0 < 2$, while the correlation energy curve has a maximum at a point near $r_0 = 2$. For $r_0 > 6$, the curves asymptotically reach their values of the free case, in this region all curves remain almost constant.